

# DUOX2 participates in skin aging induced by UVB in HSF2 cells by activating NF- $\kappa$ B signaling

XIAOQING XIAO, MINGHUAN HUANG, CHUNYAN FAN and FUGUO ZUO

Department of Dermatology, Shanghai East Hospital, Tongji University School of Medicine, Shanghai 200120, P.R. China

Received May 27, 2020; Accepted October 30, 2020

DOI: 10.3892/etm.2020.9588

**Abstract.** Skin and in particular photoaging or premature aging, are caused by a variety of factors, including hormone imbalance and exposure to ultraviolet radiation. The aim of the present study was to explore the roles of Dual oxidase 2 (DUOX2) and related NF- $\kappa$ B signals in skin photoaging. Cell models of photoaging were constructed by irradiating human skin fibroblast lines (HSF2) with ultraviolet B (UVB) of different doses (0, 15, 30 and 60 mJ/cm<sup>2</sup>). The cell counting kit-8 (CCK8) was used to determine cell proliferation. Flow cytometry was used to determine the production of reactive oxygen species (ROS). A biochemical method was used to determine the content of hydrogen peroxide, and the quantitative PCR (qPCR) was used to determine the expression of matrix metalloproteinase 2 (MMP2), matrix metalloproteinase 9 (MMP9), Col-I and  $\alpha$ -SMA in the cells. Enzyme-linked immunosorbent assay (ELISA) was used to determine the expression of tumor necrosis factor- $\alpha$  (TNF- $\alpha$ ) and interleukin-6 (IL-6). Western blot analysis was performed to determine the expression of DUOX2, p65 and p-p65. The results showed that UVB irradiation dose- and time-dependently inhibited the proliferation of HSF2 cells. Cellular inflammatory response, ROS production and hydrogen peroxide increase was promoted. Col-I and  $\alpha$ -SMA were downregulated, MMP2 and MMP9 were upregulated, and the phosphorylation of NF- $\kappa$ B p65 was promoted. The above indicators were all reversed by interference with DUOX2. Overexpression of DUOX2 has an effect that is similar to UVB irradiation, but the effects can be significantly weakened by NF- $\kappa$ B inhibitor, NAC. Upregulation of DUOX2 expression plays a crucial role in UVB-induced aging of HSF2 cells. The specific mechanism is related to the promotion of ROS production and cellular inflammatory response and activation of NF- $\kappa$ B signals.

## Introduction

Skin aging is caused by a variety of factors, including hormone imbalance and some metabolic pathway disorders, especially ultraviolet radiation (1). Photoaging refers to premature aging of skin due to long-term exposure of the skin to ultraviolet radiation (2). Of the three wavelengths of ultraviolet rays, ultraviolet B (UVB) (280-320 nm) is considered the root cause of skin photoaging. It can penetrate the epidermis to the dermis (3). Long-term ultraviolet radiation, especially UVB radiation, would give rise to the reduction of skin collagen fibers and abnormal elastic fiber deposition. The manifestations are capillary dilatation, erythrocyte sedimentation, pachulosis, dermatochalasis, and wrinkle (4).

Human dermal fibroblasts maintain skin thickness and elasticity by producing extracellular matrix (ECM) (5). UV radiation, especially UVB radiation, can result in skin photoaging. It can induce apoptosis of keratinocytes (3,6) and reactive oxygen species (ROS)-mediated inflammatory response (7). UV radiation upregulates the activity of matrix metalloproteinases (MMPs) via mitogen-activated protein kinase (MAPK) and NF- $\kappa$ B signaling pathways (8). MMPs can specifically degrade almost all types of ECM, such as Col-I, and Col-III, which play a pivotal role in skin photoaging (9). In many studies on skin photoaging, excessive generation of ROS is considered as the most important reason and therapeutic target (10). Excessive ROS activates NF- $\kappa$ B, leading to the release of inflammatory factors including tumor necrosis factor- $\alpha$  (TNF- $\alpha$ ), interleukin-1 $\beta$  (IL-1 $\beta$ ) and interleukin-6 (IL-6) (11,12). It also induces the expression of ECM-degrading enzyme, MMPs, which finally results in oxidative damage to cells (13).

Dual oxidase 2 (DUOX2) is an important NADPH oxidase catalytic subunit that regulates the production of ROS (14,15). It causes cellular inflammatory response by mediating epidermal keratinocytes by promoting the activation of NF- $\kappa$ B signals and inducing the upregulation of IL-8 and CCL20 (15). This suggests that DUOX2 may play a crucial role in UVB-induced photoaging and inflammatory response. There are no related reports at present, and the specific mechanism of action is still under investigation. Therefore, in this study, UVB was used to irradiate human skin fibroblast lines (HSF2) to construct cell models of photoaging. Then DUOX2 overexpression and interference were used in the treatment. The aim of the study was to

---

*Correspondence to:* Dr Fuguo Zuo, Department of Dermatology, Shanghai East Hospital, Tongji University School of Medicine, 150 Jimo Road, Pudong, Shanghai 200120, P.R. China  
E-mail: glbv77@163.com; zfg3792@easthospital.cn

**Key words:** photoaging, DUOX2, ROS, NF- $\kappa$ B, inflammatory response

explore the function of DUOX2 in the photoaging process and the role of NF- $\kappa$ B signals in this process.

## Materials and methods

**Cell culture and UVB radiation.** Skin fibroblasts (HSF2) were purchased from the Shanghai Institute of Biochemistry and Cell Biology (SIBCB; Chinese Academy of Sciences). The study was approved by the Ethics Committee of Shanghai East Hospital, Tongji University School of Medicine.

HSF2 cells were resuscitated and cultured in Dulbecco's modified Eagle's medium (DMEM; Hyclone) containing 10% fetal bovine serum (FBS; Life Technologies) under 5% CO<sub>2</sub> at 37°C. The cells were harvested and washed three times with sterile phosphate-buffered saline (PBS). The cells were evenly distributed in an uncovered culture dish, and irradiated with a UVB lamp (Haining Lei Top Lighting Co., Ltd.) in a biosafety cabinet at room temperature. The ultraviolet irradiation intensity was verified by an ultraviolet intensity detector (Deshengxing Technology Co., Ltd.). The irradiation distance was set to 15 cm, and UVB irradiation doses for different groups were 0 (treated in the dark), 15, 30 and 60 mJ/cm<sup>2</sup>, respectively. After each irradiation, the cells were collected by centrifugation at 1100–1200 × g at room temperature for 3 min and resuspended in sterile PBS. After repeated washing three times, they were finally resuspended in culture medium and cultured under the aforementioned conditions. The cells were irradiated with UVB for 3 days, 1 h each time, once a day. Finally, the cells and supernatant cultures were collected after irradiation for 0, 24, 48 and 72 h, respectively.

**Radiation dose selection.** UVB of different doses (0, 15, 30 and 60 mJ/cm<sup>2</sup>) was, respectively, used to irradiate human skin fibroblast (HSF2) cell lines. The cells and supernatants were then collected using the aforementioned methods after UVB irradiation. Subsequently, the proliferation of cells at 0, 12, 24 and 48 h after UVB irradiation was determined using a Cell Counting Kit-8 (CCK-8) (SABBioTech) as per the protocol. At 48 h after UVB irradiation, the ROS content of the cells was detected by flow cytometry. In addition, the content of hydrogen peroxide in the cells was determined using a hydrogen peroxide detection kit (Jiancheng Bioengineering). The expression of TNF- $\alpha$  and IL-6 in the cells was determined referring to the method of enzyme-linked immuno-sorbent assay (ELISA) kit (Cell Signaling Technology). Furthermore, the expression of MMP2, MMP9, Col-I, and  $\alpha$ -SMA in the cells was detected using quantitative PCR (qPCR), and the expression of DUOX2, p65 and p-p65 was detected using western blot analysis.

**Effects of DUOX2 overexpression on HSF2 cells.** DUOX2 overexpression and interference lentivirus vectors were constructed by JRDun Biotech, and sequences and primers are shown in Table I. Recombinant lentiviruses were produced and amplified in 293 cell packaging according to previous methods (16). The virus supernatant was diluted to required concentration in culture medium and then added to the monolayer HSF2 cells at the logarithmic phase. After 24-h incubation in DMEM medium with 10% fetal bovine serum at 37°C with 5% CO<sub>2</sub>, the relative mRNA and protein expression of DUOX2

in ADSCs was detected by reverse transcriptase-quantitative PCR and western blot analysis.

Three groups were established for the experiment: the empty vector group, the DUOX2 overexpression group, and the DUOX2 overexpression + NAC group (5 mM, NF- $\kappa$ B inhibitor). Cells in each group were cultured for 24 h under normal conditions, and then the cells and supernatant were harvested. Finally, the content of hydrogen peroxide in the cells was determined using the biochemical method. The expression of TNF- $\alpha$  and IL-6 in the cells was determined by ELISA. Furthermore, the expression of MMP2, MMP9, Col-I and  $\alpha$ -SMA in the cells was detected using qPCR, and the expression of DUOX2, p65 and p-p65 was detected using western blot analysis.

**Effects of DUOX2 interference on UVB-induced aging of HSF2 cells.** Five groups were set up for the experiment: the control group, the UVB irradiation group, the empty vector group, the UVB + siDUOX2 group, and the UVB + NAC group. Cells in the control group were given dark treatment, and cells in the remaining four groups were irradiated with 30 mJ/cm<sup>2</sup> UVB and transfected with corresponding virus vectors or given NAC treatment. Cells and supernatant were collected 24 h after treatment. Finally, the content of hydrogen peroxide in the cells was determined using the biochemical method. The expression of Col-I,  $\alpha$ -SMA, TNF- $\alpha$  and IL-6 in the cells was determined using ELISA. In addition, the expression of DUOX2, MMP2, MMP9, p65 and p-p65 in cells was determined using western blot analysis.

**ROS detection.** According to a previous report, DCFH-DA analysis was used to evaluate the ROS content (17). Briefly, HSF2 cells (1 × 10<sup>6</sup>/ml) were cultured with 5  $\mu$ M 2',7'-dichlorofluorescein diacetate (DCFH-DA) at 37°C for 20 min (mixed forward and backward every 3 min). DCFH-DA (non-fluorescent) entered cells and hydrolyzed into cell impermeable and non-fluorescent DCFH. ROS in the cells oxidized DCFH into highly fluorescent dichlorofluorescein (DCF). Green fluorescence intensity was proportional to ROS content. After the cells were stimulated at 480 nm, the DCF fluorescence was detected at 525 nm via a flow cytometer (Becton Dickinson). The result was expressed as the ratio of fluorescence intensity of HSF2 cells in other groups to that of the normal group.

**RT-qPCR.** The mRNA expression was detected by reverse transcriptase-quantitative PCR (RT-qPCR). Total RNA (2  $\mu$ g per sample) was extracted and reverse transcribed into cDNA using a reverse transcription kit (Thermo Fisher Scientific, Inc.). The obtained cDNA was taken as a template and analyzed using RT-qPCR with an RT-PCR instrument (ABI-7300; Applied Biosystems) and SYBR-Green reagent (Thermo Fisher Scientific, Inc.).

Primers for RT-qPCR (Table II) were designed in Primer 5.0 software and synthesized by JRDun Biotech. Using glyceraldehyde-3-phosphate dehydrogenase (GAPDH) gene expression as the internal reference, the relative mRNA expression of each sample was detected by the 2<sup>- $\Delta\Delta$ Cq</sup> method (18) and relative quantitative analysis.  $\Delta\Delta$ Cq = (Cq, target gene of the treatment group - Cq, internal reference gene of the treatment

Table I. DUOX2 overexpression and interference primers.

Genes	Primer sequence (5'-3')
DUOX2 overexpression	Forward: 5'-CCCAAGCTTATGCTCCGTGCAAGACCAG-3' Reverse: 5'-CGGAATTCAGAAAGTTCTCATAGTGGTGC-3'
DUOX2 interference (si-1)	Forward: 5'-CGCUAUGACGGCUGGUUUUATT-3' Reverse: 5'-UAAACCAGCCGUCAUAGCGTT-3'
DUOX2 interference (si-2)	Forward: 5'-GGAGUGAUCUCAACCCUAATT-3' Reverse: 5'-UUAGGGUUGAGAUCACUCCTT-3'
DUOX2 interference (si-3)	Forward: 5'-GGAAUGGGCUGUUCUCCAATT-3' Reverse: 5'-UUGGAGAACAGCCCAUUCCTT-3'
Interference control (si-NC)	Forward: 5'-UUCUCCGAACGUGUCACGUTT-3' Reverse: 5'-ACGUGACACGUUCGGAGAATT-3'

Table II. Primers used for RT-qPCR.

Genes	Primer sequence (5'-3')
MMP2 NM_001127891.2	Forward: 5'-TTGGTGGGAACCTCAGAAG-3' Reverse: 5'-TTGCGGTTCATCATCGTAG-3'
MMP9 NM_004994.2	Forward: 5'-GTGGCACCACCACAACATCAC-3' Reverse: 5'-CGCGACACCAAACTGGATGAC-3'
Col-I NM_000088.4	Forward: 5'-TCTTTGACCAACCGAACATGAC-3' Reverse: 5'-TTGATTGCTGGGCAGACAATAC-3'
$\alpha$ -SMA NM_001141945.2	Forward: 5'-CCGGGACATCAAGGAGAAAC-3' Reverse: 5'-CGATGAAGGATGGCTGGAAC-3'
DUOX2 NM_014080.4	Forward: 5'-CGAGTTTGCCGAGTCCC-3' Reverse: 5'-AAGCCATTCTCATCCAGGTC-3'
GAPDH NM_001256799.2	Forward: 5'-AATCCCATCACCATCTTC-3' Reverse: 5'-AGGCTGTTGTCATACTTC-3'

group)-(Cq, target gene of the control group-Cq, internal reference gene of the control group).

**Western blot analysis.** Total protein of each sample was extracted using Cell Protein Extraction Reagent (Thermo Fisher Scientific, Inc.), and its content was determined by a bicinchoninic acid (BCA) detection kit (Thermo Fisher Scientific, Inc.). The protein (30  $\mu$ g/sample) was separated by 10% sodium-dodecyl-sulfate-polyacrylamide gel-electrophoresis (SDS-PAGE), and then transferred to a polyvinylidene difluoride (PVDF) membrane. Subsequently, the membrane was sealed with 5% skim milk at 25°C for 1 h, and then cultured with appropriate primary antibodies: MMP2 (1:1,000; cat. no. ab92536; Abcam), MMP9 (1:1,000; cat. no. ab76003; Abcam), p65 (1:500; cat. no. sc-71675; Santa Cruz Biotechnology), p-p65 (1:2,000; cat. no. ab183559; Abcam), DUOX2 (1:400; cat. no. ab170308; Abcam) or GAPDH (1:2,000; no. 5174; Cell Signaling Technology). The membrane was incubated with HRP-conjugated IgG secondary antibody (1:1,000; cat. no. A0208; Beyotime Institute of Biotechnology) at 25°C for 1 h. Finally, the

protein band was detected by an electrochemiluminescence (ECL) detection kit (Beyotime Institute of Biotechnology). The film was scanned using a Tanon-5200 chemiluminescent Gel Image System Ver. 4.00 (Tanon Science & Technology Co., Ltd.). GAPDH was used as control.

**Statistical analyses.** The data were expressed as mean  $\pm$  standard deviation (n=3), and analyzed using the variance analysis and Duncan's multiple range test. Data differences were analyzed using SPSS 20.0 software (SPSS Inc.). P<0.05 indicates a significant difference.

## Results

**Radiation dose selection.** In this part, UVB of different doses (0, 15, 30 and 60 mJ/cm<sup>2</sup>) was used to irradiate human skin fibroblast lines (HSF2) for 48 h, separately. The results showed that, low-dose UVB exerted no effect on the proliferation of HSF2 cells, but with the extension of time and increase of dose, UVB significantly inhibited proliferation (Fig. 1A). In addition, 48 h after treatment, UVB

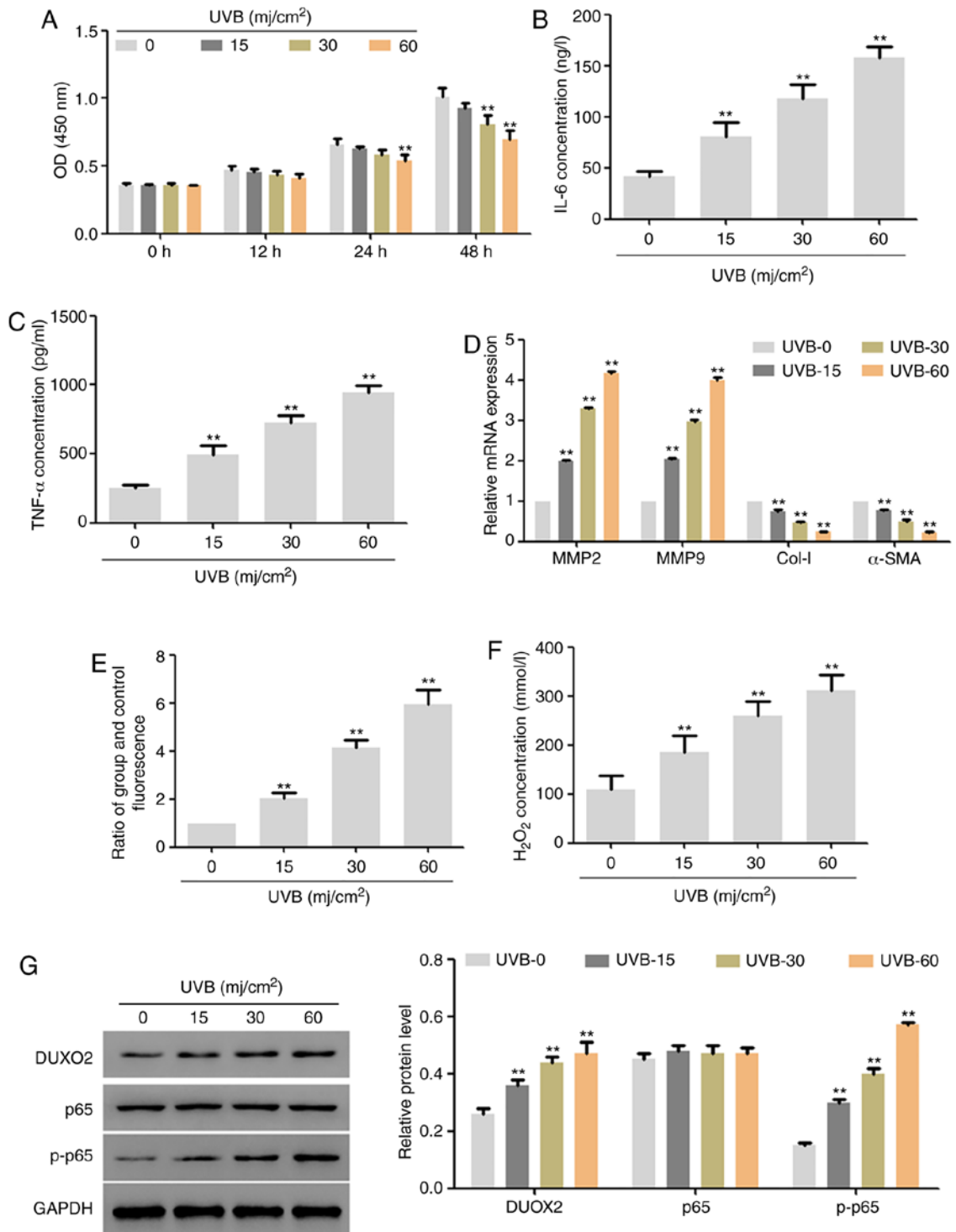


Figure 1. Effects of UVB treatment on HSF2 cells. UVB inhibited the proliferation of (A) HSF2 cells. UVB induced the increase of (B) IL-6 and (C) TNF- $\alpha$ . (D and E) UVB promoted the production of ROS production and increase of hydrogen peroxide content. UVB upregulated the mRNA expression of MMP2 and MMP9 and downregulated the mRNA expression of Col-I and  $\alpha$ -SMA (F). UVB induced the protein expression of DUOX2 and promoted the phosphorylation of NF- $\kappa$ B p65 (G). \*\*P<0.01 vs. the control group.

significantly upregulated the expression of IL-6 and TNF- $\alpha$  (Fig. 1B and C) and the mRNA expression of MMP2 and MMP9, significantly downregulated the mRNA expression of Col-I and  $\alpha$ -SMA (Fig. 1D), and also upregulated the ROS content and hydrogen peroxide content (Fig. 1E and F). Moreover, UVB upregulated the protein expression of DUOX2 and p-p65 in a dose-dependent manner (Fig. 1G).

According to the above results and the effects of UVB on cell proliferation, we used 30 mj/cm<sup>2</sup> UVB to treat cells for 48 h in the subsequent experiments.

*Efficacy identification of DUOX2 interference and overexpression vectors.* In the subsequent experiments, lentivirus vectors with DUOX2 interference and overexpression were

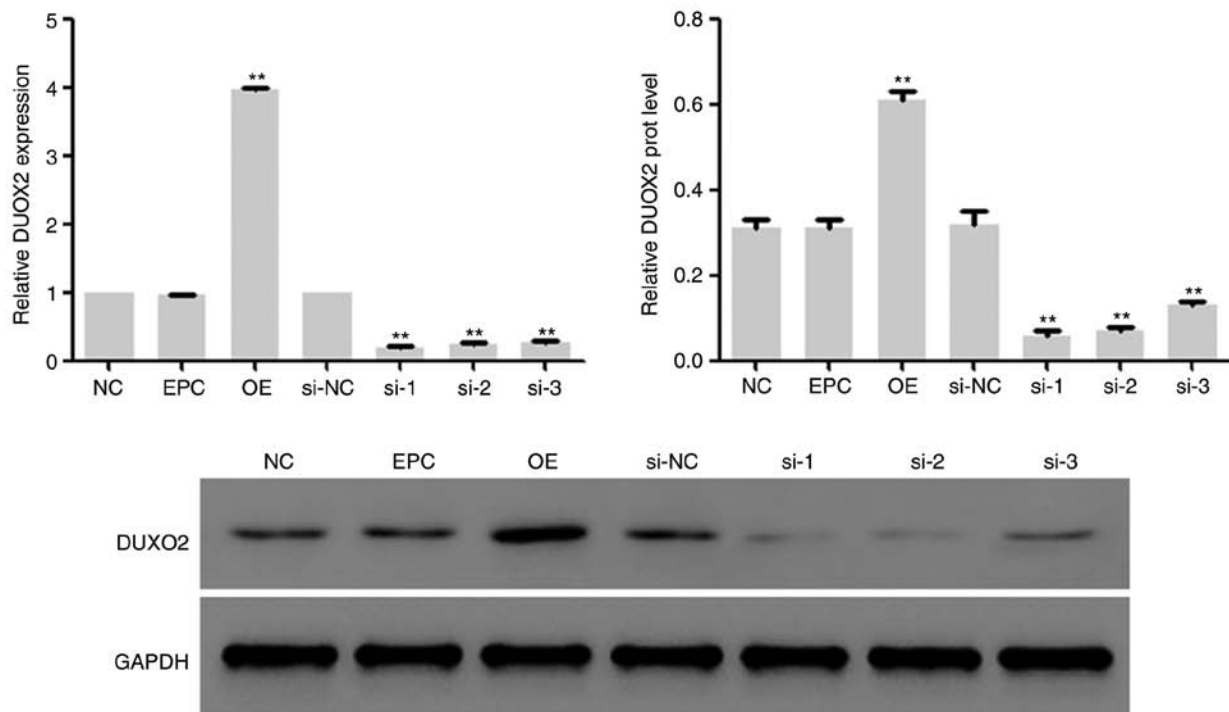


Figure 2. mRNA and protein expression of DUOX2 after DUOX2 interference and overexpression. \*\* $P < 0.01$  vs. the empty vector group or the si-NC group.

constructed, and transfected into HSF2 cells, followed by 48-h incubation in DMEM medium with 10% fetal bovine serum at 37°C with 5% CO<sub>2</sub>. Then the mRNA and protein expression of DUOX2 in the cells was determined, and it was found that the expression of DUOX2 in HSF2 cells was inhibited by DUOX2 interference and upregulated by DUOX2 overexpression (Fig. 2). The lentivirus vectors corresponding to interference sequence 2 (si-2) was used for subsequent interference experiments.

**Effects of DUOX2 overexpression on HSF2 cells.** In the subsequent experiments, the effects of DUOX2 overexpression on HSF2 cells were determined, and HSF2 cells were treated with NF- $\kappa$ B inhibitor NAC to explore the role of NF- $\kappa$ B signals in this process (19). As shown in Fig. 3, the expression of IL-6 and TNF- $\alpha$  was upregulated by DUOX2 overexpression, but the upregulation was inhibited by NAC (Fig. 3A and B). In addition, the same trend was found in ROS production and hydrogen peroxide content in the cells (Fig. 3D and E). The mRNA and protein expression of MMP2 and MMP9, as well as the phosphorylation level of p65 were induced by DUOX2, but downregulated by NF- $\kappa$ B inhibitor NAC (Fig. 3C and F). The mRNA expression of Col-I and  $\alpha$ -SMA was inhibited by DUOX2 overexpression, but the inhibition was weakened by NF- $\kappa$ B (Fig. 3C).

**Effects of DUOX2 interference on UVB-induced aging of HSF2 cells.** The effects of DUOX2 interference on HSF2 cells under UVB (30 mJ/cm<sup>2</sup>) irradiation were further studied. We found that DUOX2 interference significantly inhibited the UVB-induced upregulation of TNF- $\alpha$  and IL-6 and downregulation of Col-I and  $\alpha$ -SMA (Fig. 4A-D). ROS production and hydrogen peroxide content were induced by UVB and the induction was inhibited by DUOX2 interference

(Fig. 4E and F). In addition, the protein expression of MMP2 and MMP9 and the phosphorylation level of p65 were upregulated by UVB, but the upregulation was weakened by DUOX2 interference (Fig. 4G).

## Discussion

Long-term ultraviolet irradiation is considered to be the primary cause of skin damage, and it leads to photoaging (1). Photoaged skin is clinically characterized with pachulosis, dermatochalasis, and wrinkle, which are closely related to the disorder of collagen fibers and the reduction of collagen content (20,21). UVB radiation mediates the phosphorylation of protein kinases by inducing ROS-mediated MAPK and NF- $\kappa$ B signaling pathways, further inducing cellular inflammatory response (8). Chronic and low-grade inflammation is also considered a major feature of the aging process. This phenomenon is called 'inflamm-aging'. Inflamm-aging plays an important role in many age-related diseases such as type 2 diabetes, Alzheimer's disease, cardiovascular disease, weakness, skeletal muscle reduction, osteoporosis and skin aging (22,23). In addition, ROS can lead to the upregulation of expression and activity of MMPs, which is closely related to collagen degradation in photoaged skin (24,25). This conclusion is confirmed by our study. UVB radiation can induce the production of ROS, increase the hydrogen peroxide content in HSF2 cells and inhibit cell proliferation. It can also induce the activation of NF- $\kappa$ B signals and promote the increase of inflammatory factors (TNF- $\alpha$  and IL-6). Furthermore, UVB radiation can also induce the expression of DUOX2. Although UVB radiation induces an increase in DUOX2 and p65 phosphorylation levels, the rate of increase in p65 phosphorylation levels is higher, which indicates that UVB radiation-induced NF- $\kappa$ B

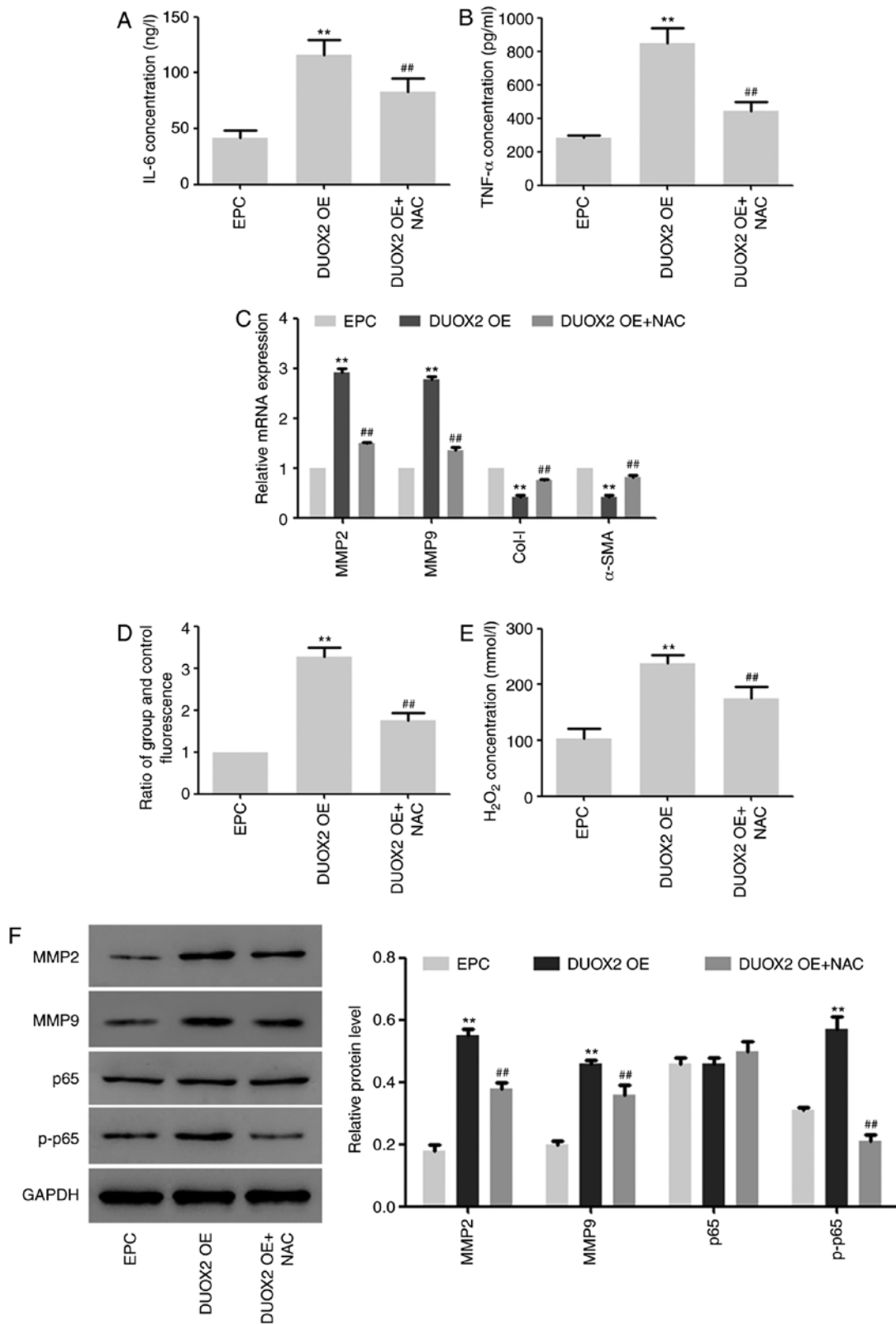


Figure 3. Effects of DUOX2 overexpression combined with NF- $\kappa$ B inhibitor treatment on HSF2 cells. (A and B) The increase of IL-6 and TNF- $\alpha$  levels was induced by DUOX2 overexpression, but was decreased by treatment of DUOX2 overexpression combined with NAC. (C) Effects of DUOX2 overexpression combined with NF- $\kappa$ B inhibitor treatment on the expression of MMP2, MMP9, Col-I and  $\alpha$ -SMA in HSF2 cells. (D and E) Effects of DUOX2 overexpression combined with NF- $\kappa$ B inhibitor treatment on ROS production and hydrogen peroxide content in cells. DUOX2 overexpression induced MMP2 and MMP9 and phosphorylation of p65, but the effect was inhibited by combined treatment with (F) NAC. \*\*P<0.01 vs. the empty vector group. ##P<0.01 vs. the overexpression group.

phosphorylation involves multiple factors and may be the result of multiple cascading signals.

DUOX2 is a subtype of NOX NADPH oxidase, and the defect in DUOX2 is manifested by congenital hypothyroidism (26).

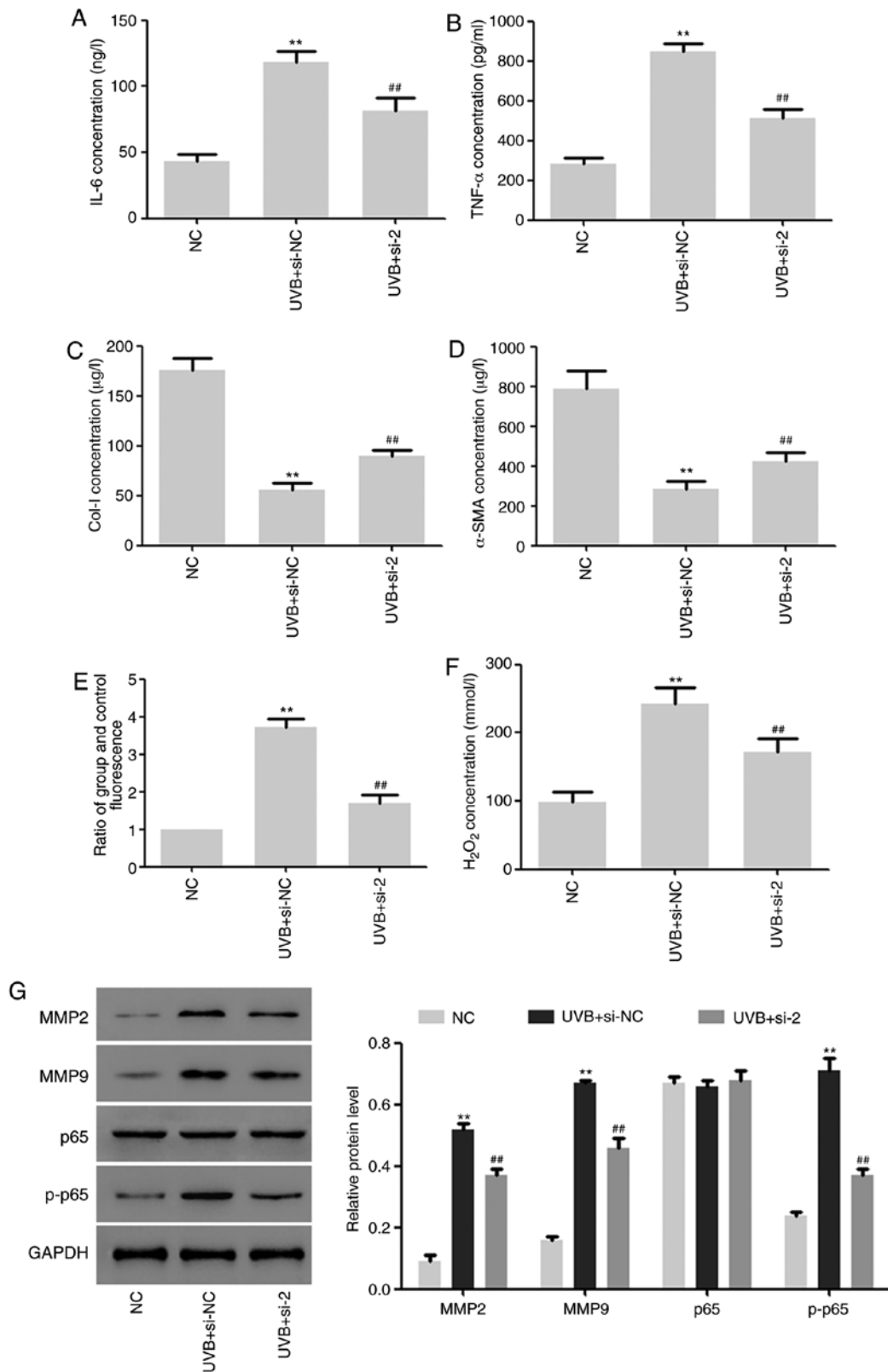


Figure 4. Effects of DUOX2 interference on UVB-induced aging of HSF2 cells. (A-D) DUOX2 interference inhibited UVB-induced upregulation of TNF- $\alpha$  and IL-6 and downregulation of Col-I and  $\alpha$ -SMA. (E and F) DUOX2 interference inhibited UVB-induced ROS production and upregulation of hydrogen peroxide content. (G) The protein expression of MMP2 and MMP9 and the phosphorylation level of p65 were upregulated by UVB treatment, but weakened by DUOX2 interference. \*\* $P < 0.01$  vs. the NC group. ## $P < 0.01$  vs. the UVB + si-NC group.

In addition, it is reported that DUOX2 could mediate the production of ROS to induce epithelial-mesenchymal transition in 5-fluorouracil-resistant human colon cancer cells (27).

The DUOX2-mediated production of hydrogen peroxide, DUOX2-mediated DNA damage and inflammatory response play important roles in gastrointestinal tumors and prostate

tumors. This effect may be realized by activating NF- $\kappa$ B signals (28). In addition, findings of correlation studies between NADPH oxidase ROS and human aging revealed that properly controlling the activity of physiological redox signals of NADPH oxidase for cell homeostasis maintenance may be a therapeutic strategy to promote healthy aging (29). The latest research has found that dioxygenases (DUOXes), which are usually prominently expressed in the epithelial lineage, are usually inhibited by epigenetic mechanisms in epithelial-derived cancers (30). DUOXes also mediate the regulation of Th1 and Th2 immune cells on the production of respiratory tract ROS in the host defense response (31). These mechanisms may directly or indirectly involve the photodamage mechanism that leads to photoaging and skin cancer. It suggests that DUOX2 plays an essential role in skin photoaging, especially UVB-induced photoaging. However, there are no relevant reports thus far. Results of the present study have shown for the first time, to the best of our knowledge, the role of DUOX2 in UVB-induced aging of HSF2 cells. DUOX2 induces the production of ROS, increases the content of hydrogen peroxide in HSF2 cells. It also promotes the cellular inflammatory response, the expression of MMP2 and MMP9, and the degradation of collagens, and activates NF- $\kappa$ B signals. The correlation between MMP and phosphorylation (p-p65) is disproportionate. The reason may be that NAC is a specific inhibitor of NF- $\kappa$ B, and overexpression of DUOX2 may also regulate the expression of MMP through other signaling pathways such as MAPK signaling (32). However, this effect is significantly weakened by NF- $\kappa$ B inhibitor NAC. In addition, in HSF2 cells irradiated by UVB, interference with DUOX2 can reduce UVB-induced ROS production, cellular inflammatory response and NF- $\kappa$ B overactivation.

To sum up, the upregulation of DUOX2 expression plays a crucial role in UVB-induced aging of HSF2 cells, and the specific mechanism is related to the promotion of ROS production, cellular inflammatory response, and activation of NF- $\kappa$ B signals.

### Acknowledgements

Not applicable.

### Funding

No funding was received.

### Availability of data and materials

The datasets used and/or analyzed during the present study are available from the corresponding author on reasonable request.

### Authors' contributions

XX and FZ conceived, designed the study and drafted the manuscript. XX, MH and CF collected, analyzed and interpreted the experimental data. XX revised the manuscript for important intellectual content. All authors read and approved the final manuscript.

### Ethics approval and consent to participate

The study was approved by the Ethics Committee of Shanghai East Hospital, Tongji University School of Medicine.

### Patient consent for publication

Not applicable.

### Competing interests

The authors declare that they have no competing interests.

### References

1. Krutmann J, Bouloc A, Sore G, Bernard BA and Passeron T: The skin aging exposome. *J Dermatol Sci* 85: 152-161, 2017.
2. Huang CY, Lin YT, Kuo HC, Chiou WF and Lee MH: Compounds isolated from *Eriobotrya deflexa* leaves protect against ultraviolet radiation B-induced photoaging in human fibroblasts. *J Photochem Photobiol* 175: 244-253, 2017.
3. Nichols JA and Katiyar SK: Skin photoprotection by natural polyphenols: Anti-inflammatory, antioxidant and DNA repair mechanisms. *Arch Dermatol Res* 302: 71-83, 2010.
4. Goldman MP, Weiss RA and Weiss MA: Intense pulsed light as a nonablative approach to photoaging. *Dermatol Surg* 31: 1179-1187, 2005.
5. Mora Huertas AC, Schmelzer CE, Hoehenwarter W, Heyroth F and Heinz A: Molecular-level insights into aging processes of skin elastin. *Biochimie* 128-129: 163-173, 2016.
6. Lei X, Liu B, Han W, Ming M and He YY: UVB-Induced p21 degradation promotes apoptosis of human keratinocytes. *Photochem Photobiol Sci* 9: 1640-1648, 2010.
7. Duncan FJ, Martin JR, Wulff BC, Stoner GD, Tober KL, Oberyszyn TM, Kusewitt DF and Van Buskirk AM: Topical treatment with black raspberry extract reduces cutaneous UVB-induced carcinogenesis and inflammation. *Cancer Prev Res (Phila)* 2: 665-672, 2009.
8. Sharma SD, Meeran SM and Katiyar SK: Dietary grape seed proanthocyanidins inhibit UVB-induced oxidative stress and activation of mitogen-activated protein kinases and nuclear factor-kappaB signaling in in vivo SKH-1 hairless mice. *Mol Cancer Ther* 6: 995-1005, 2007.
9. Fisher GJ, Datta SC, Talwar HS, Wang ZQ, Varani J, Kang S and Voorhees JJ: Molecular basis of sun-induced premature skin ageing and retinoid antagonism. *Nature* 379: 335-339, 1996.
10. Poon F, Kang S and Chien AL: Mechanisms and treatments of photoaging. *Photodermatol Photoimmunol Photomed* 31: 65-74, 2015.
11. Yokoyama T, Komori A, Nakamura M, Takii Y, Kamihira T, Shimoda S, Mori T, Fujiwara S, Koyabu M, Taniguchi K, *et al*: Human intrahepatic biliary epithelial cells function in innate immunity by producing IL-6 and IL-8 via the TLR4-NF-kappaB and -MAPK signaling pathways. *Liver Int* 26: 467-476, 2006.
12. Orlando A, Cazzaniga E, Tringali M, Gullo F, Becchetti A, Minniti S, Taraballi F, Tasciotti E and Re F: Mesoporous silica nanoparticles trigger mitophagy in endothelial cells and perturb neuronal network activity in a size- and time-dependent manner. *Int J Nanomedicine* 12: 3547-3559, 2017.
13. Matsumura Y and Ananthaswamy HN: Toxic effects of ultraviolet radiation on the skin. *Toxicol Appl Pharmacol* 195: 298-308, 2004.
14. Bedard K and Krause KH: The NOX family of ROS-generating NADPH oxidases: Physiology and pathophysiology. *Physiol Rev* 87: 245-313, 2007.
15. Song H, Zhao H, Yang L, Li L, Zhang T, Pan J, Meng Y, Shen W and Yuan Y: *Achyranthes bidentata* polypeptides promotes migration of Schwann cells via NOX4/DUOX2-dependent ROS production in rats. *Neurosci Lett* 696: 99-107, 2019.
16. Luo J, Tang M, Huang J, He BC, Gao JL, Chen L, Zuo GW, Zhang W, Luo Q, Shi Q, *et al*: TGFbeta/BMP type I receptors ALK1 and ALK2 are essential for BMP9-induced osteogenic signaling in mesenchymal stem cells. *J Biol Chem* 285: 29588-29598, 2010.



17. Caldefie-Chézet F, Walrand S, Moinard C, Tridon A, Chassagne J and Vasson MP: Is the neutrophil reactive oxygen species production measured by luminol and lucigenin chemiluminescence intra or extracellular? Comparison with DCFH-DA flow cytometry and cytochrome c reduction. *Clin Chim Acta* 319: 9-17, 2002.
18. Livak KJ and Schmittgen TD: Analysis of relative gene expression data using real-time quantitative PCR and the 2(-Delta Delta C(T)) method. *Methods* 25: 402-408, 2001.
19. Ko EY, Cho SH, Kwon SH, Eom CY, Jeong MS, Lee W, Kim SY, Heo SJ, Ahn G, Lee KP, *et al*: The roles of NF- $\kappa$ B and ROS in regulation of pro-inflammatory mediators of inflammation induction in LPS-stimulated zebrafish embryos. *Fish Shellfish Immunol* 68: 525-529, 2017.
20. Hsieh HY, Lee WC, Senadi GC, Hu WP, Liang JJ, Tsai TR, Chou YW, Kuo KK, Chen CY and Wang JJ: Discovery, synthetic methodology, and biological evaluation for antiphotoreactive activity of bicyclic[1,2,3]triazoles: In vitro and in vivo studies. *J Med Chem* 56: 5422-5435, 2013.
21. Wlaschek M, Tantcheva-Poór I, Naderi L, Ma W, Schneider LA, Razi-Wolf Z, Schüller J and Scharffetter-Kochanek K: Solar UV irradiation and dermal photoaging. *J Photochem Photobiol B* 63: 41-51, 2001.
22. Zhuang Y and Lyga J: Inflammaging in skin and other tissues-the roles of complement system and macrophage. *Inflamm Allergy Drug Targets* 13: 153-161, 2014.
23. Fulop T, Larbi A, Dupuis G, Le Page A, Frost EH, Cohen AA, Witkowski JM and Franceschi C: Immunosenescence and inflamm-aging as two sides of the same coin: Friends or foes? *Front Immunol* 8: 1960, 2017.
24. PLOS ONE Editors: Retraction: Anti-wrinkle effect of magnesium lithospermate B from salvia miltiorrhiza BUNGE: Inhibition of MMPs via NF- $\kappa$ B signaling. *PLoS One* 14: e0216473, 2019.
25. Staniforth V, Huang WC, Aravindaram K and Yang NS: Ferulic acid, a phenolic phytochemical, inhibits UVB-induced matrix metalloproteinases in mouse skin via posttranslational mechanisms. *J Nutr Biochem* 23: 443-451, 2012.
26. Buvelot H, Jaquet V and Krause KH: Mammalian NADPH oxidases. *Methods Mol Biol* 1982: 17-36, 2019.
27. Kang KA, Ryu YS, Piao MJ, Shilnikova K, Kang HK, Yi JM, Boulanger M, Paolillo R, Bossis G, Yoon SY, *et al*: DUOX2-mediated production of reactive oxygen species induces epithelial mesenchymal transition in 5-fluorouracil resistant human colon cancer cells. *Redox Biol* 17: 224-235, 2018.
28. Wu Y, Konaté MM, Lu J and Makhlof H: IL-4 and IL-17A cooperatively promote hydrogen peroxide production, oxidative DNA damage, and upregulation of dual oxidase 2 in human colon and pancreatic cancer cells. *J Immunol* 203: 2532-2544, 2019.
29. Ewald CY: Redox signaling of NADPH oxidases regulates oxidative stress responses, immunity and aging. *Antioxidants (Basel)* 7: 130, 2018.
30. Little AC, Sulovari A, Danyal K, Heppner DE, Seward DJ and van der Vliet A: Paradoxical roles of dual oxidases in cancer biology. *Free Radic Biol Med* 110: 117-132, 2017.
31. Harper RW, Xu C, Eiserich JP, Chen Y, Kao CY, Thai P, Setiadi H and Wu R: Differential regulation of dual NADPH oxidases/peroxidases, Duox1 and Duox2, by Th1 and Th2 cytokines in respiratory tract epithelium. *FEBS Lett* 579: 4911-4917, 2005.
32. Moldogazieva NT, Mokhosoev IM, Feldman NB and Lutsenko SV: ROS and RNS signalling: Adaptive redox switches through oxidative/nitrosative protein modifications. *Free Radic Res* 52: 507-543, 2018.